Polym. Bull. (2017) 74:4607–4618
DOI 10.1007/s00289-017-1978-2

ORIGINAL PAPER

Compatibility, mechanical and thermal properties of GAP/P(EO-*co*-THF) blends obtained upon a urethane-curing reaction

Yajin Li[1] · Jie Li[1] · Song Ma[1] · Yunjun Luo[1]

Received: 27 July 2016 / Revised: 8 March 2017 / Accepted: 13 March 2017 /
Published online: 16 March 2017

Abstract A series of cross-linked glycidyl azide polymer with poly(ethylene oxide-*co*-tetrahydrofuran) (GAP/P(EO-*co*-THF)) blends were prepared by varying the relative weight ratios of GAP to P(EO-*co*-THF) using poly-isocyanate mixed curing system (N100/TDI), and by varying the [NCO]/[OH] ratios to find the effects of curing agents on mechanical properties. The compatibility, thermal features and morphological studies of GAP/P(EO-*co*-THF) polymer networks were described by equilibrium phase diagram, differential scanning calorimeters (DSC) together with thermogravimetric analysis (TGA), scanning electron microscopy (SEM), respectively. The equilibrium phase figure of the partial miscibility system for GAP/P(EO-*co*-THF) shows that the system has a lower critical solution temperature (LCST). In addition, the DSC and TGA results indicate that the content of two components is gradually approaching, and the glass transition temperatures of GAP/P(EO-*co*-THF) blends are less than those of the pure GAP and P(EO-*co*-THF) polymers, and the initial decomposition temperature and the maximum decomposition rate temperature have greatly increased. Furthermore, the thermal decomposition behavior indicates that the thermal stabilities are improved and the physical entangled networks are strengthened. Moreover, the scanning electron microscopy (SEM) images show the GAP/P(EO-*co*-THF) blends form a certain polymer alloy structure, which is the reason for the improved thermal stabilities and the strengthened networks.

Keywords GAP · Compatibility · Mechanical properties · Thermal decomposition

✉ Yunjun Luo
yjluo@bit.edu.cn

[1] School of Materials Science and Engineering, Beijing Institute of Technology, Beijing 100081, China

Introduction

The high-energy rocket propellants with high ballistic performance and excellent mechanical properties are continuously developing because of their application in the aerospace industry and long-range missiles [1, 2]. Nitrate ester plasticized polyether (NEPE) propellants are polymer-bonded high-energy cross-linking propellants, which combine both the advantages of composite solid propellant and double base propellant (XLDB). As one of the important binders for NEPE propellants, Poly(Ethylene Oxide-*co*-Tetrahydrofuran) (P(EO-*co*-THF)) polymer demonstrates excellent properties as shown in the application of rocket propellants, such as low glass transition temperature, high flexibility, hydrolytic stability and resistance to solvents [3, 4]. Therefore, based on its outstanding features, the P(EO-*co*-THF) contained propellants have excellent comprehensive properties; however, the P(EO-*co*-THF) polymer is an inert binder, which leads to a defect that most of the energy of NEPE propellants only comes from solid filler such as RDX, aluminum powder and ammonium perchlorate (AP). This reason limits the energy performance improvement for the propellants.

According to the literatures, glycidyl azide polymer (GAP) has been considered as a distinctive candidate binder used in advanced composite solid propellants formulations [5–7]. GAP is a unique binder with high density and positive heat of formation of $+117.2\ \mathrm{kJ{\cdot}mol^{-1}}$ and is compatible with high energetic oxidizers like ammonium dinitramide (ADN) [8, 9]. However, the highly energetic azide groups($C\text{-}N_3$) along the GAP polymer chain as pendent groups make the intermolecular force smaller [10–12] and the poor flexibility of backbone usually results in inferior mechanical behaviors for the solid propellants [13]. A facile way to improve the binder performance is to copolymerize it with flexible molecular, so GAP with vinyl or flexible monomers may solve these problems to some extent [14]. In recent years, GAP is generally used as co-binder or as a plasticizer with poly(ethylene glycol) (PEG), poly(caprolactone) (PCL), tetra hydro furan (THF), ethylene oxide (EO) and hydroxyl terminated poly (butadiene) (HTPB) though the results were unsatisfactory [15–17]. Byoung Sun Min and Eva Landsem applied themselves to the study on polyether-type block copolymer binder and ammonium nitrate propellants, and they found that polyether copolymer binders could improve the mechanical properties and reduce the values of T_g for the co-polyurethane networks [18–20]. Mathew et al. investigated the thermomechanical and morphological characteristics of the cross-linked GAP-HTPB networks, however, due to the incompatibility between HTPB and GAP, their blended propellants still exhibited poor mechanical properties [21, 22]. To avoid phase separation occurring when using GAP with other ingredients in composite solid propellants, we tried to present other flexible molecular such as P(EO-*co*-THF) polymer.

Generally speaking, the binders were cross-linked by diisocyanates like toluene diisocyanate (TDI), isophorone diisocyanate (IPDI) and polyisocyanate such as Desmodur N-100 [23, 24]. The selection of the curing agent is important for energetic materials application. Aromatic and aliphatic diisocyanates vary in their reactivity with respect to the primary or secondary nature of the hydroxyl functional

groups [25]. This paper use both aromatic and aliphatic isocyanates like TDI and N-100.

In this paper, a series of networks have been prepared by varying the relative weight ratios of GAP to P(EO-*co*-THF) using poly-isocyanate mixed curing system (N100/TDI), and by varying the [NCO]/[OH] ratios to find the effects of curing agents on mechanical properties. The thermal features were studied by Differential scanning calorimeters (DSC) and thermogravimetric analysis (TGA), and the morphological studies of GAP/P(EO-*co*-THF) polymer networks were described by scanning electron microscopy (SEM). This paper also detailed the miscibility of GAP and P(EO-*co*-THF) polymer by partially miscible liquid–liquid binary phase diagram theory.

Experimental

Materials and measurements

GAP (OH value: 0.53 $mmol \cdot g^{-1}$) with an average molecular weight about 3600 $g \cdot mol^{-1}$, P(EO-*co*-THF) (OH value: 0.44 $mmol \cdot g^{-1}$) with an average molecular weight about 4038 $g \cdot mol^{-1}$. Both of the hydroxyl-terminated polymers were purchased from Hubei Aviation Institute of Chemical Technology and purified by vacuum drying.

The curing agents were N100 and toluene diisocyanate (TDI). Desmodur N100 poly-isocyanate and toluene diisocyanate have average molecular weight of 728 and 174 $g \cdot mol^{-1}$, respectively. Triphenyl bismuth (TPB) was used as curing catalyst in a 0.5 wt% solution in dioctyl sebacate (DOS).

The stress–strain test of the elastomers was measured using a tensile testing machine (Instron-6022, Shimadzu Co. Ltd) at a constant strain rate of 100 mm/min at room temperature. The dimensions of the samples were 20 mm (neck area length) × 4 mm (width) × 2 mm (thickness). DSC testing was made over the temperature range from −100 to 150 °C on Mettler DSC1 with a 10 °C/min heating rate in a nitrogen atmosphere (40 mL/min). TGA analysis was performed on Mettler TGA-STAR system at heating rate of 10 °C/min from 30–600 °C in a nitrogen atmosphere (40 mL/min). Scanning Electron Microscopy (SEM) was obtained with a Hitachi TM3000 cold field emission scanning electron microscope set with a 15.0 kV acceleration voltage.

Preparation of GAP/P(EO-*co*-THF) polymer networks

All the reagents were dried overnight in a vacuum oven at 60 °C before use. Cured GAP/P(EO-*co*-THF) films were prepared from diisocyanates and by varying [NCO]/[OH] ratios to find the effects of curing agents concentration on mechanical properties. The [NCO]/[OH] ratio (R value) varied from 1.1 to 1.9 for the purpose of the paper. The required amount of TPB (0.3%) was added every time and the mix was stirred, followed by degassing in a vacuum oven at 40 °C. The mixture was finally poured into a Teflon mold and cured under 60 °C for 7 days.

Results and discussion

Compatibility studies on GAP/P(EO-*co*-THF) blends

GAP is a polymer with polyether backbone and the presence of the azide moiety in the polymer make it polar in nature, while P(EO-*co*-THF) binder is a flexible molecule with methylene and ether backbone. Hence, GAP and P(EO-*co*-THF) may not be miscible and phase separation will occur for the blends. In the present study, we drew the equilibrium phase figure centering on partial miscibility system of GAP/P(EO-*co*-THF) blending liquid on the basis of the partially miscible liquid–liquid binary phase diagram theory. First, different ratios of GAP/P(EO-*co*-THF) were mixed in test tube. Then, kept them undisturbed for a certain time after being dispersed until obvious phase separation phenomenon occured. According to the concentration of two-phase solutions which were confirmed by the peak change of $-N_3$ and C–H in FTIR, the ratios of upper and lower solutions could be calculated. A series of ratios could be obtained at different weight ratio of GAP and different temperature, and then drew the phase diagram, as shown in Fig. 1.

Figure 1 shows the system has a lower critical solution temperature (LCST). When the initial ratios of GAP/P(EO-*co*-THF) are in the metastable or homogeneous region, the mixture can be stable without phase separation. However, if the initial ratios of GAP to P(EO-*co*-THF) polymer are 55–65% of W_{GAP}, the mixture would directly pass over the region from metastable zone to Two-phase region. This phenomenon manifests that the phase separation velocity of the blending is affected by ambient temperature and solution concentration.

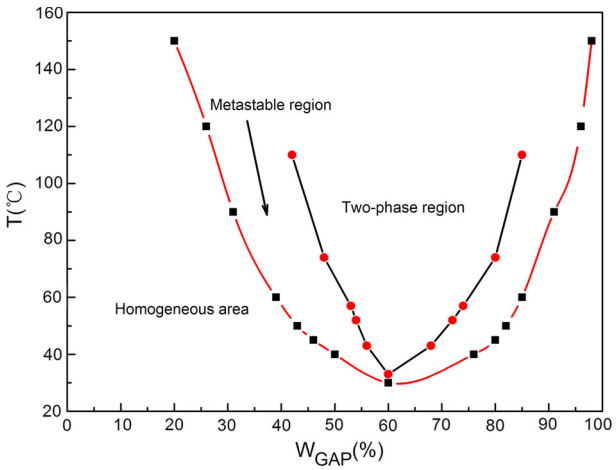

Fig. 1 Partial miscibility binary liquid phase diagram of GAP/P(EO-*co*-THF) (7 days)

Mechanical properties of cured GAP/P(EO-*co*-THF) blends

The mechanical property of polymeric network is known to be strongly dependent on the structure of elastic network. To study the influence of the composites system on the mechanical property for polymeric network, a series of uniaxial tensile tests for GAP/P(EO-*co*-THF) composites at room temperature were carried out. Figure 2 shows the stress–strain data of GAP/P(EO-*co*-THF) composites at different curing ratios ([NCO]/[OH]) when the proportion of GAP and P(EO-*co*-THF) is 50:50. The tensile strength and elongation at break of the GAP/P(EO-*co*-THF) composites gradually increase with an escalation of the *R* value ([NCO]/[OH]) from 1.1 to 1.6 and then decrease until the *R* value continuously increases up to 1.9. Meanwhile, the elastic modulus maintains around 0.05–0.025 MPa. When the *R* value is 1.6, the σ_b and ε_b of the GAP/P(EO-*co*-THF) film reach the maximum values of 2.15 MPa and 598%, respectively. As the [NCO]/[OH] ratios of the composites increases, the excess –NCO groups remains in the cross-linked network, forming some pendent chain which leads to a decline in mechanical properties. In addition, it also indicates that the increase of –NCO groups could not increase the mechanical properties, as the formation of the side reaction reduces the tensile strength and elongation of GAP/P(EO-*co*-THF) elastomers.

Figure 3 shows the influence of GAP/P(EO-*co*-THF) ratios on mechanical properties, in which the R value of composites is 1.6. The results indicate that by increasing the weight ratio of GAP, the tensile strength steadily increases from 1.95 to 2.58 MPa and then decreases to 0.25 MPa, while breaking elongation gradually

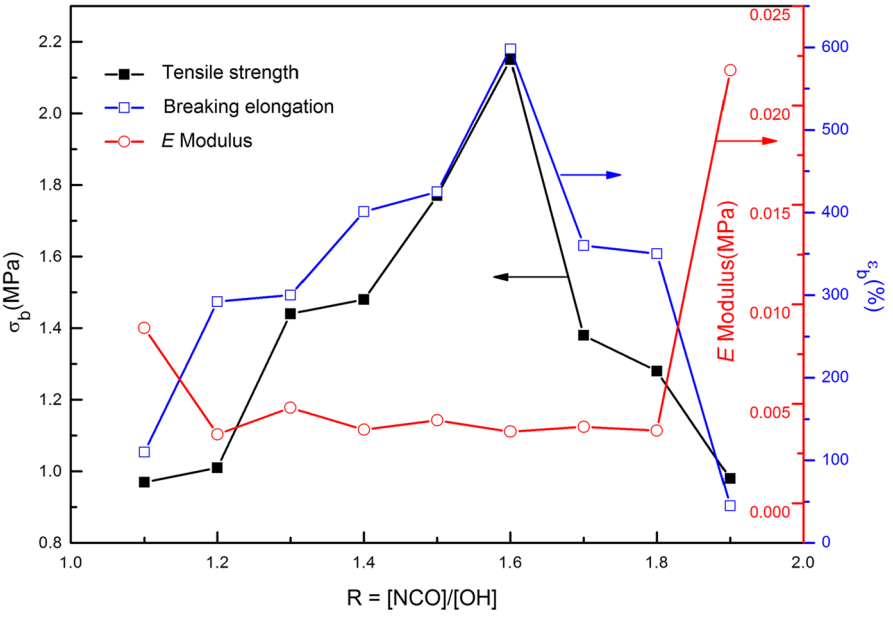

Fig. 2 Effects of the curing ratios (NCO/OH) on the tensile strength (σ_b) and breaking elongation (ε_b) of 50:50 wt% GAP/P(EO-*co*-THF) composites

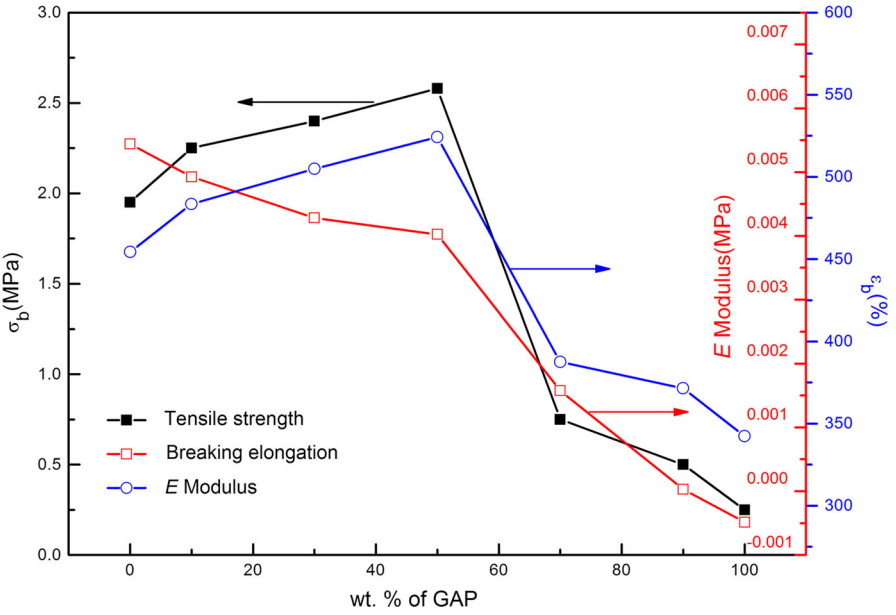

Fig. 3 Effects of wt% of GAP on the tensile strength (σ_b) and breaking elongation (ε_b) of GAP/P(EO-*co*-THF) composites ([NCO]/[OH] value is 1.6)

decreases from 520 to 290%. The elastic modulus decreases following the weight ratio of GAP. The maximum tensile strength 2.58 MPa with 465% elongation is achieved with wt 50% of GAP, and the decrease of the mechanical properties may be due to the stratification of the GAP and P(EO-*co*-THF) networks. In addition, the elasticity of GAP is inhibited by the azido groups and the chain flexibility is extremely restricted beyond wt 50% of GAP.

Herein, we also chose a curing ratio [NCO]/[OH] of 1.6 and 50:50% of GAP/P(EO-*co*-THF) to investigate the influence of N100/TDI ratios. Figure 4 shows that by increasing the weight ratio of N100, tensile strength first increases from 1.12 to 1.59 MPa and then decreases to 1.02 MPa, while breaking elongation gradually decreases from 695 to 150%. An extensive increase in tensile strength and decrease in breaking elongation occur during sequential polymerization. In the curing systems, Desmodur N100 is the only cross-linking agent which has functionality greater than 2. As the N100 weight ratios increases, tensile strength gradually increases at the expense of elongation due to the formation of stiffer structures, which restricts chain mobility. As a result of this, the matrix takes more loads with less breaking elongation. In general, more cross-linking points result in higher tensile strength, however, beyond 40% N100, the defects of network structure and stiffer networks are highly formed before solidification so the tensile strength and elongation at break progressively drops up to 1.02 MPa and 150%, respectively. Moreover, the *E* modulus increases from 0.03 to 0.14 following the weight ratio of N100.

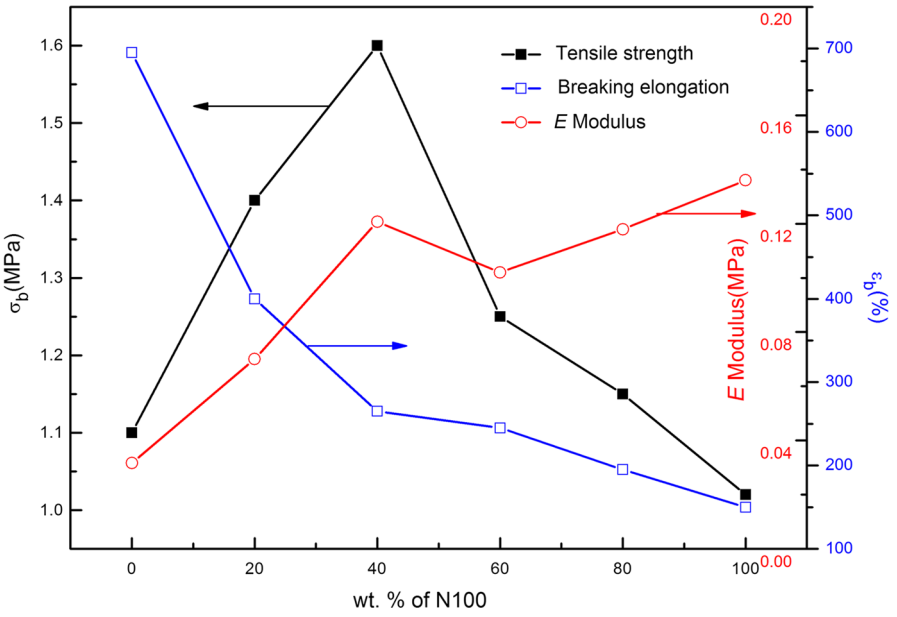

Fig. 4 Effects of wt% of N100 on the tensile strength (σ_b) and breaking elongation (ε_b) of GAP/P(EO-*co*-THF) composites (50:50 wt% of GAP/P(EO-*co*-THF), [NCO]/[OH] value is 1.6)

Glass transition temperature

Figure 5 shows the DSC traces of the GAP/P(EO-*co*-THF) composites with different weight ratios, and Table 1 summarizes the glass transition temperature (T_g) from the DSC traces. According to Table 1, it shows three glass transition temperatures, indicating that the GAP/P(EO-*co*-THF) blends form two kinds of soft segments. The glass transition temperatures (T_g) of the pure GAP and P(EO-*co*-THF) networks are found to be about −42 and −79 °C, respectively (Fig. 6). Furthermore, as the content of two components is gradually approaching, the two glass transition temperatures of GAP/P(EO-*co*-THF) blending elastomers soft segments locate in between pure GAP and P(EO-*co*-THF) polymers. With the increase in weight ratio of GAP before 30%, only one T_g is observed and slightly increases from −79.1 to −78.4 °C. When the GAP weight ratio reaches 50%, it shows two glass transition temperatures at about −77.5 and −42.5 °C, which may be a result of micro phase separation but fortunately has synergistic mechanical properties. Based on the equilibrium phase figure, with 50:50% GAP/P(EO-*co*-THF) weight ratio in metastable region, the copolymer networks may form polymer alloy rather than irrelevant phases, in which physical entanglements, interlocking of polymer networks and reduction of gap between cross-linked points coexist. The glass transition temperature (T_{g3}) of hard segment reduces with GAP content decreasing. On the whole, this phenomenon is consistent with the glass temperature characteristics of not completely incompatible polymer alloy. Except for the partial miscibility nature between GAP and P(EO-*co*-THF) binders, the results also

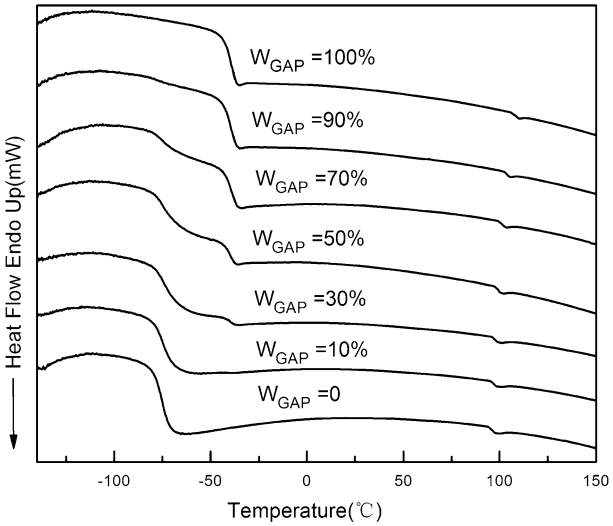

Fig. 5 DSC traces of the GAP/P(EO-*co*-THF) composites with various content of GAP ([NCO]/[OH] value is 1.6, 40:60 wt% of N100/TDI)

suggests that GAP/P(EO-*co*-THF) networks form polymer alloy, instead of forming two irrelevant phases.

Thermal decomposition properties

It is essential to study the decomposition behavior of polymeric propellant materials, because it plays a crucial role in the combustion behavior of the composite solid propellants, and the data are closely associated with vital performance parameters like heat of explosion, detonation energy and velocity [26, 27]. The cured GAP/P(EO-*co*-THF) networks were prepared from GAP whose content varied from 0 to 100%. In the TGA-DTG analysis of GAP/P(EO-*co*-THF) blends, a three-step degradation behavior is observed. The representative TG-DTG curves of GAP/P(EO-*co*-THF) blends are presented in Figs. 7 and 8. The first stage of peak decomposition temperatures starts around 244–257 °C with an approximate mass weight loss of 32%, which is caused by the nitrogen elimination from the

Table 1 DSC data of the GAP/P(EO-*co*-THF) composites with various content of GAP

Sample	T_{g1} (°C)	T_{g2} (°C)	T_{g3} (°C)
W_{GAP}-100	–	−43.0	105.4
W_{GAP}-90	–	−42.9	101.3
W_{GAP}-70	−77.2	−42.6	100.1
W_{GAP}-50	−77.5	−42.5	99.8
W_{GAP}-30	−78.4	−42.1	98.6
W_{GAP}-10	−78.8	–	97.1
W_{GAP}-0	−79.1	–	96.3

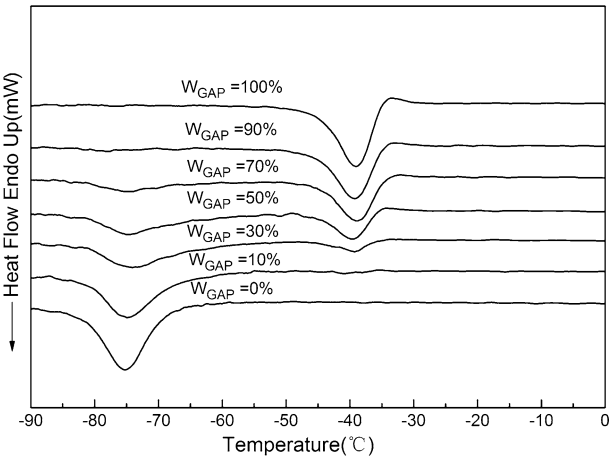

Fig. 6 The first derivative heat flow rate of the GAP/P(EO-*co*-THF) composites with various contents of GAP ([NCO]/[OH] value is 1.6, 40:60 wt% of N100/TDI)

azido groups of GAP while the pure P(EO-*co*-THF) film does not have weight loss at this temperature. The second decomposition stage of composites involves the backbone degradation of carbamate and allophanate in the temperature range of 300–310 °C with weight loss of 19%. The temperature of the third decomposition stage ranges from 360 to 420 °C on account of the hydrocarbon backbone and the remaining cyclized products decomposition of the main chains belonging to P(EO-*co*-THF) and GAP. After the third decomposition stage, the residue left behind is around 2–23%. As the content of two components is gradually approaching, the initial decomposition temperature and the maximum decomposition rate

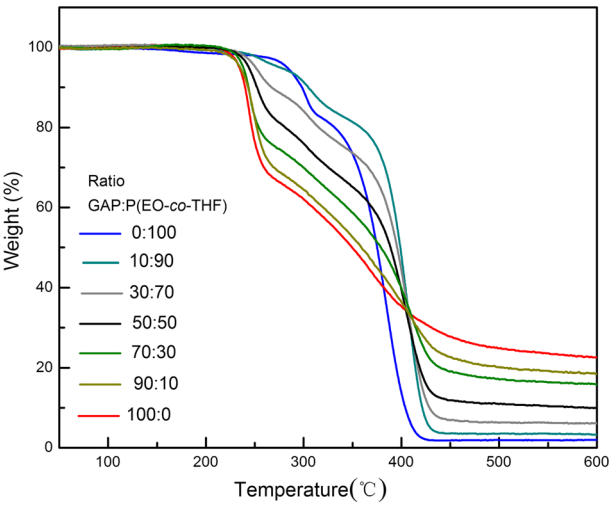

Fig. 7 TG diagram of GAP/P(EO-*co*-THF) composites with various content of GAP ([NCO]/[OH] value is 1.6, 40:60 wt% of N100/TDI)

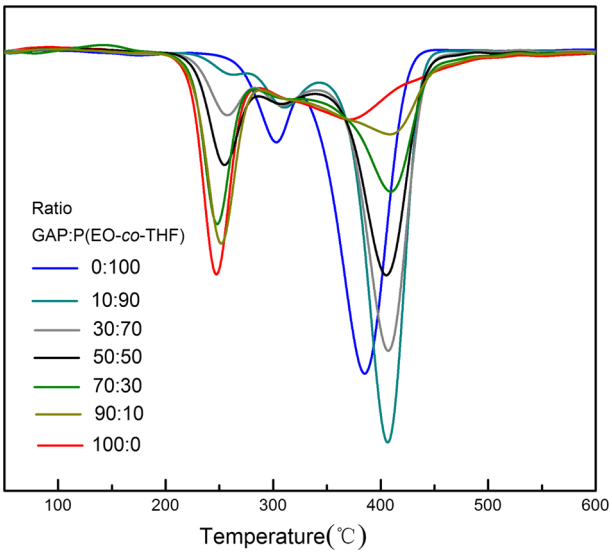

Fig. 8 DTG traces of GAP/P(EO-*co*-THF) composites with various content of GAP ([NCO]/[OH] value is 1.6, 40:60 wt% of N100/TDI)

temperature have greatly increased to a certain extent compared to pure GAP and P(EO-*co*-THF) films. It indicates that the improvement of composite thermal stability is due to the compact network formation and the physical entanglement increase.

Morphology analysis

Figure 9 depicts the morphological characteristics of the fractured surfaces of the GAP/P(EO-*co*-THF) networks with SEM analysis. The surface of the network is

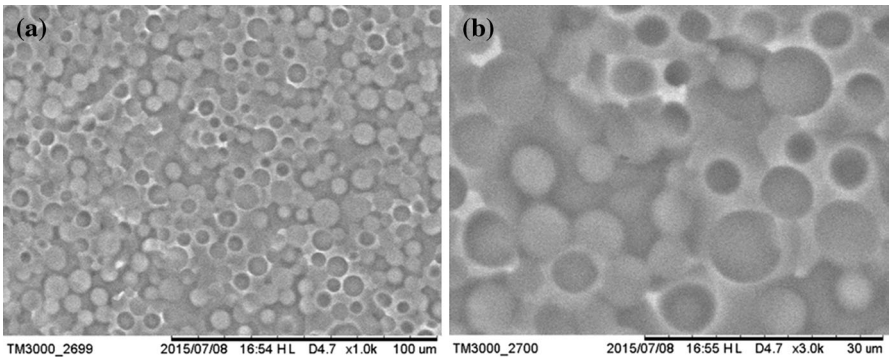

Fig. 9 SEM images of the fractured surface of GAP/P(EO-*co*-THF) networks prepared at 50:50 wt% of GAP/P(EO-*co*-THF), [NCO]/[OH] value is 1.6, 40:60 wt% of N100/TDI. **a** GAP/P(EO-*co*-THF) cured using N100/TDI, **b** the local amplification of blends

obtained from the sample in liquid nitrogen via freeze fracturing. The micrographs given in Fig. 9a shows the two continuous phases of both networks from GAP and P(EO-*co*-THF), which is the spherical network structure resulted by the low temperature crystallization of GAP polymer and based on P(EO-*co*-THF) network matrix. Wherein, polymer chains emerge to penetrate inward and outward over one another in polymer matrix showing good compatibility. The morphology also proves that the composites form a certain polymer alloy structure.

Conclusions

The equilibrium phase figure of partial miscibility system with GAP/P(EO-*co*-THF) shows that the system has a lower critical solution temperature (LCST). When the initial ratio of GAP/P(EO-*co*-THF) is in the metastable or homogeneous region, the mixture can be stable without phase separation. At the same time, the DSC and TG-DTG studies of GAP/P(EO-*co*-THF) blends indicate that the content of two components is gradually approaching, and the glass transition temperatures of GAP/P(EO-*co*-THF) elastomers are less than those of pure GAP and P(EO-*co*-THF) polymers, and the initial decomposition temperature and the maximum decomposition rate temperature have greatly increased to a certain extent. These results are consistent with the characteristics of not completely incompatible polymer alloy. Except for the partial miscibility nature between GAP and P(EO-*co*-THF) binders, the GAP/P(EO-*co*-THF) networks form polymer alloy, instead of forming two irrelevant phases. In addition, the SEM images also show that the composites form a certain polymer alloy structure.

A series of GAP/P(EO-*co*-THF) cross-linked networks have been prepared by varying the relative weight ratios of GAP and P(EO-*co*-THF), and the maximum tensile strength of 2.58 MPa with 465% elongation has been achieved with 50% of GAP. The mechanical properties of cured GAP/P(EO-*co*-THF) blends are found that when the [NCO]/[OH] ratio is 1.6, the σ_b and ε_b reach the maximum values of 2.15 MPa and 598%, respectively.

The results show that the cross-linked GAP/P(EO-*co*-THF) blends possess better mechanical properties and the phase separation is avoided by the kinetics through adjusting the appropriate proportion and the curing temperature of GAP/P(EO-*co*-THF) composites to form a certain polymer alloy structure. This property provides convenience for the adjustment of both technology and energy performance of high-energy rocket propellants.

References

1. Kanti Sikder A, Reddy S (2013) Review on energetic thermoplastic elastomers (ETPEs) for military science. Propellants Explos Pyrotech 38(1):14–28
2. Badgujar DM, Talawar MB, Asthana SN (2008) Advances in science and technology of modern energetic materials: an overview. J Hazard Mater 151(2):289–305

3. Consaga JP, French DM (1971) Properties of hydroxyl-terminated polybutadiene-urethane systems. J Appl Polym Sci 15(12):2941–2956
4. Hovetborn T, Holscher M, Keul H, Höcker H (2006) Poly (ethylene oxide-*co*-tetrahydrofuran) and Poly (propylene oxide-*co*-tetrahydrofuran): synthesis and thermal degradation. Rev Roum Chim 51(7/8):781
5. Nazare A, Asthana S, Singh H (1992) Glycidyl azide polymer (GAP)-an energetic component of advanced solid rocket propellants-a review. J Energ Mater 10(1):43–63
6. Frankel M, Grant L, Flanagan J (1992) Historical development of glycidyl azide polymer. J Propul Power 8(3):560–563
7. Beckstead MW, Puduppakkam KV, Thakre P, Yang V (2007) Modeling of combustion and ignition of solid-propellant ingredients. Prog Energy Combust Sci 33(6):497–551
8. Manu SK, Varghese TL, Mathew S (2009) Studies on structure property correlation of cross-linked glycidyl azide polymer. J Appl Polym Sci 114(6):3360–3368
9. Cerri S, Bohn MA, Menke K (2014) Characterization of ADN/GAP-Based and ADN/desmophen-based propellant formulations and comparison with AP analogues. Propellants Explos Pyrotech 39(2):192–204
10. Sekkar V, Bhagawan SS, Prabhakaran N (2000) Polyurethanes based on hydroxyl terminated polybutadiene: modelling of network parameters and correlation with mechanical properties. Polymer 41(18):6773–6786
11. Selim K, Özkar S, Yilmaz L (2000) Thermal characterization of glycidyl azide polymer (GAP) and GAP-based binders for composite propellants. J Appl Polym Sci 77(3):538–546
12. Gaur B, Lochab B, Choudhary V (2003) Azido polymers-energetic binders for solid rocket propellants. J Macromol Sci Part C Polym Rev 43(4):505–545
13. Stacer RG, Husband DM (1991) Molecular structure of the ideal solid propellant binder. Propellants Explos Pyrotech 16(4):167–176
14. Mohan YM, Raju MP, Raju KM (2005) Synthesis and characterization of GAP-PEG copolymers. Int J Polym Mater 54(7):651–666
15. Menke K, Heintz T, Schweikert W (2009) Formulation and properties of ADN/GAP propellants. Propellants Explos Pyrotech 34(3):218–230
16. Min BS (2008) Characterization of the plasticized GAP/PEG and GAP/PCL block copolyurethane binder matrices and its propellants. Propellants Explos Pyrotech 33(2):131–138
17. Davenas A (2003) Development of modern solid propellants. J Propul Power 19(6):1108–1128
18. Min BS, Ko SW (2007) Characterization of segmented block copolyurethane network based on glycidyl azide polymer and polycaprolactone. Macromol Res 15(3):225–233
19. Min BS, Baek G, Ko SW (2007) Characterization of polyether-type GAP and PEG blend matrices prepared with varying ratios of different curatives. J Ind Eng Chem 13(3):373–379
20. Landsem E, Jensen TL, Hansen FK et al (2012) Neutral polymeric bonding agents (NPBA) and their use in smokeless composite rocket propellants based on HMX-GAP-BuNENA. Propellants Explos Pyrotech 37(5):581–591
21. Manu SK, Varghese TL, Joseph MA et al (2004) Physical, mechanical and morphological characteristics of chain modified GAP and GAP-HTPB binder matrices. In: International Annual Conference-fracunhofer Institut fur Chemische Technologie
22. Mohan YM, Raju KM (2005) Synthesis and characterization of HTPB-GAP cross-linked co-polymers. Des Monomers Polym 8(2):159–175
23. Panda SP, Sahu SK, Sadafule DS et al (2000) Role of curing agents on decomposition and explosion of glycidyl azide polymers. J Propul Power 16(4):723–725
24. Bui VT, Ahad E, Rheaume D et al (1996) Energetic polyurethanes from branched glycidyl azide polymer and copolymer. J Appl Polym Sci 62(1):27–32
25. Mathew S, SeK Manu, TeL Varghese (2008) Thermomechanical and morphological characteristics of cross-linked GAP and GAP–HTPB networks with different diisocyanates. Propellants Explos Pyrotech 33(2):146–152
26. Herder G, Weterings F, de Klerk W (2003) Mechanical analysis on rocket propellants. J Therm Anal Calorim 72(3):921–929
27. Krabbendam-La Haye E, de Klerk W, Miszczak M et al (2003) Compatibility testing of energetic materials at TNO-PML and MIAT. J Therm Anal Calorim 72(3):931–942